AIAA AVIATION Forum
June 27-July 1, 2022, Chicago, IL & Virtual
AIAA AVIATION 2022 Forum
10.2514/6.2022-3788

A frequency-domain-inspired reformulation of the unsteady vortex lattice method

Jiayao Yan* and John T. Hwang†
University of California, San Diego, La Jolla, CA, 92093

The unsteady vortex lattice method (UVLM) is a low-fidelity tool for modeling unsteady, inviscid, irrotational, and incompressible flows. The standard formulation of the UVLM method includes a time-stepping process, which presents a challenge for vectorizing the model, and thus increases the cost of computing derivatives, e.g., for large-scale multidisciplinary optimization. This paper addresses this challenge by proposing a frequency-domain-inspired reformulation of the UVLM that evolves the wake geometry to be close to a force-free wake through an objective function in the optimization problem. A verification case of the frequency-domain-inspired model is presented, followed by a rotary-wing and a plunging-wing aerodynamic analysis and wake geometry computation. The wake contraction is captured for the rotary-wing case. Further investigation of the plunging wing case needs to be performed.

I. Introduction

The vortex lattice method (VLM) is a low-fidelity numerical method that models aerodynamic performance quantities such as lift, drag, and pitching moment of given lifting surfaces [1, 2]. It is derived from analytical solutions to incompressible potential flow theory, based on the assumption of an irrotational velocity field, with viscous forces neglected. The steady-state VLM has been widely used and integrated as the aerodynamic disciplinary model for large-scale multidisciplinary design optimization (MDO) of aircraft [3–6]. The unsteady vortex lattice method (UVLM) is an extension of the VLM that can model time-dependent flows.

The time-dependent nature of the UVLM introduces complexity and efficiency issues in high-dimensional MDO applications. Recent developments in the MDO community have significantly reduced the implementation complexity of large-scale MDO algorithms by leveraging modeling frameworks (e.g., OpenMDAO [7]) that enable adjoint-based derivative computation in a modular way. However, the most commonly used form of the UVLM applies a time-marching procedure that introduces difficulties when computing derivatives for gradient-based optimization. In particular, the induced velocity has to be computed at each time step to update the wake geometry for the next time step. Since the UVLM involves a time-stepping process, an ODE solver must be part of the model. However, the time-marching process in the ODE solver inhibits the use of vectorization in the model implementation, which is a critical component for efficiency in these large-scale MDO frameworks.

Previous work presented various formulations to reduce the computational cost for the UVLM. One solution is to use reduced-order modeling (ROM) methods [8–10]. Bundith et al. presented a reduced-order modeling method without static corrections based on an eigenanalysis [10]. This method has the potential to analyze unsteady flows with high efficiency. However, assuming the aerodynamic influence coefficients (AIC) are known matrices prevents the wake from evolving to form a force-free wake. Another solution is the frequency-domain VLM method by Parenteau and Laurendeau [11, 12]. Assuming the motion of the lifting surfaces is periodic, this method solves for the Fourier coefficients that parameterize the circulation strengths. Thus, only a small number of time instances within a period need be considered, instead of a large number of time steps in a time marching procedure. This method greatly reduces the computation time for lifting surfaces with periodic motions. But similar to the ROM approach, the geometry of the wake has to be prescribed.

These issues motivate the development of a new formulation of the UVLM that has lower computational cost than the time-marching-based UVLM, with a minimal sacrifice of accuracy. We make the assumption that the motion of the lifting surfaces is periodic, but allow the wake geometry to deviate from a purely periodic solution, in order to closely approximate the exact UVLM solution.

As our goal is to formulate a method to allow the wake geometry to move towards a force-free wake, we now review existing methods for computing the wake geometry. The first method is called fixed/rigid wake, which does not allow the

*PhD Student, Department of Mechanical and Aerospace Engineering, AIAA Student Member.
†Assistant Professor, Department of Mechanical and Aerospace Engineering, AIAA Member.

wake to move relative to the local undisturbed velocity. Fixed wake models do not capture wake contraction of rotors, as well as wake deformation due to interactions, which lead to a significant difference in wake geometry compared to free wake models [13]. The induced velocity evaluated on the wake is ignored. This method is used in both the ROM and frequency-domain VLM approaches mentioned previously. However, fixed wake models do not capture wake contraction in rotors, as well as wake deformation due to interactions, which lead to a significant difference in wake geometry compared to free wake models [13]. Another method is called the prescribed wake method [14, 15]. Similar to the fixed wake method, the induced velocity of the wake is not computed. But the wake geometry is prescribed using empirical equations or experimental data. Thus, this method lacks generality and requires significant knowledge input from the user, reducing the predictive power of the tool. The last approach is called the free-wake method. The free-wake method allows the wake to move with the local induced velocity. There are two schemes for the free wake method: the wake relaxation and the time-stepping method [16]. The time-stepping method is described in detail in the book written by Katz and Plotkin [17]. The wake relaxation approach was presented by Miller and Bliss [18] by considering a rotor age parameter and applying the periodic boundary condition on the wake geometry with the same age parameter.

We propose a new approach toward making the wake deformable with local velocity without time stepping. This approach is inspired by the frequency-domain formulation presented by Parenteau et al. [11]. We parameterize the wake in a parametric domain and use optimization to allow the wake to move toward a force-free direction. The following properties are present in the new formulation: 1) a general method that works well in a range of scenarios (e.g., rotor, plunging wing, and flapping wings); 2) the absence of time-stepping procedures in the algorithm; 3) a small number of degrees of freedom; 4) higher prediction accuracy than the fixed-wake method.

The paper proceeds as follows. Section II reviews the time-domain VLM and the frequency domain VLM method, which provides a background to our approach. Section III expands on the problem formulation and method. Section IV presents sample solutions to a rotary-wing and a plunging wing case. Finally, Sec. V concludes the paper and outlines the future work.

II. Background

This section reviews the time-domain vortex lattice method and the frequency-domain formulation proposed by Parenteau and Laurendeau [11].

A. Time-domain vortex lattice method

The time-domain VLM models lifting surfaces, such as wings and rotor blades, and their wakes as thin sheets of vortex rings (shown in Fig. 1).

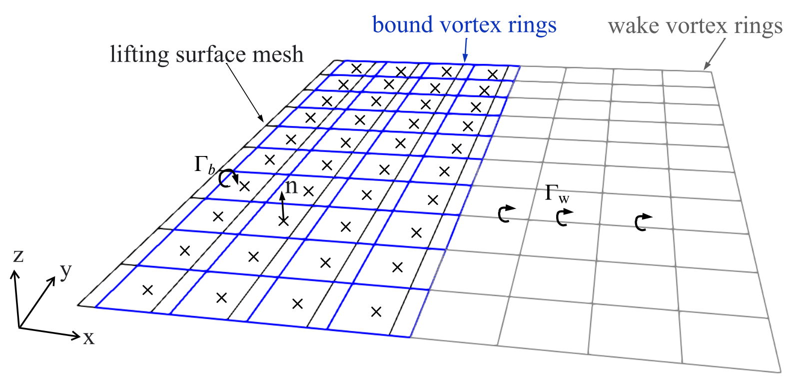

Fig. 1 Vortex ring visualization of time-domain vortex lattice method, where n is the normal vector; Γ_b and Γ_w are the bound circulation strengths and the wake circulation strengths. The cross sign denotes the collocation points located on the $\frac{3}{4}$ chord.

The VLM method is based on the assumptions of incompressible potential flow, which is given by

$$\nabla^2\Phi = 0\,, \tag{1}$$

where Φ is the fluid velocity potential. The system of equations to be solved at each time step corresponds to the flow-tangency condition

$$\boldsymbol{A}\boldsymbol{\Gamma}_{\mathrm{b}} + \boldsymbol{B}\boldsymbol{\Gamma}_{\mathrm{w}} + \boldsymbol{v} \cdot \boldsymbol{n} = 0 \,, \tag{2}$$

where $\boldsymbol{v}$ is the undisturbed flow velocity or kinematic velocity of the fluid; $\boldsymbol{n}$ is the normal vector of the bound vortex panels; $\boldsymbol{\Gamma}_{\mathrm{b}}$ and $\boldsymbol{\Gamma}_{\mathrm{w}}$ are the bound vortex circulation strengths and the wake vortex circulation strengths; and $\boldsymbol{A}$ and $\boldsymbol{B}$ are the aerodynamic influence coefficients. The flow-tangency condition enforces a zero magnitude for the fluid velocity component normal to the lifting surface. The VLM model evaluates the induced velocities on the collocation points located on $\frac{3}{4}$ chord of the lifting surface mesh (shown in Fig. 1) using the Biot–Savart law.

The forces acting on the vortex panels can be calculated using the vectorized form of the Kutta–Joukowski theorem:

$$\boldsymbol{F} = \rho\boldsymbol{\Gamma}_{\mathrm{b}}\boldsymbol{v}_{\mathrm{ind}} \times \boldsymbol{s} + \rho\frac{\partial\boldsymbol{\Gamma}_{\mathrm{b}}}{\partial t}\boldsymbol{c}\boldsymbol{v}_{\mathrm{ind}} \times \boldsymbol{s} \,, \tag{3}$$

where ρ is the density of the air; $\boldsymbol{v}_{\mathrm{ind}}$ is the induced velocities evaluated on the bound vortex collocation points; $\boldsymbol{s}$ is the bound vector; and $\boldsymbol{c}$ is a vector containing the chord lengths.

B. Frequency-domain vortex lattice method

Based on the assumptions that the motion of the lifting surfaces is periodic, the circulation strengths can be represented as

$$\boldsymbol{\Gamma}_{\mathrm{b}} = \boldsymbol{a}_0 + \sum_{k=1}^{N}[\boldsymbol{a}_{\mathrm{k}}\cos(\omega kt) + \boldsymbol{b}_{\mathrm{k}}\sin(\omega kt)] \,, \tag{4}$$

where $\boldsymbol{a}_0$, $\boldsymbol{a}_{\mathrm{k}}$, and $\boldsymbol{b}_{\mathrm{k}}$ are vectors of Fourier coefficients that parameterize the bound circulation strengths. The Fourier coefficients are then concatenated into a vector

$$\hat{\boldsymbol{\Gamma}}_{\mathrm{b}} = [\boldsymbol{a}_0, \boldsymbol{a}_1, \boldsymbol{b}_1, \ \ldots, \boldsymbol{a}_{\mathrm{k}}, \boldsymbol{b}_{\mathrm{k}}] \,. \tag{5}$$

The circulation strengths can be computed from the Fourier coefficients as

$$\boldsymbol{\Gamma}_{\mathrm{b}} = \boldsymbol{P}\hat{\boldsymbol{\Gamma}}_{\mathrm{b}} \,, \tag{6}$$

where $\boldsymbol{P}$ is a matrix containing $[1,\ \cos(\omega t),\ \sin(\omega t)]$ for the bound vortex circulations.

The wake circulation strengths are expressed as the history of the trailing-edge circulation strengths $\boldsymbol{\Gamma}_{\mathrm{TE}}$ as:

$$\boldsymbol{\Gamma}_{\mathrm{w}}(t_i) = \boldsymbol{\Gamma}_{\mathrm{TE}}(t_i - (i+1)\Delta t) \,, \tag{7}$$

where $t_i = \frac{i}{2N+1}\mathrm{T}$ is the corresponding time instance; T is the period; and N is the number of dominant frequencies. If N=1, we need to evaluate three time instances at $t_1 = \frac{1}{3}\mathrm{T}$, $t_2 = \frac{2}{3}\mathrm{T}$, and $t_3 = \mathrm{T}$ to solve for the Fourier coefficients. An example is shown in Fig. 4 that the time instances that need to be considered for a wing that moves with constant x-directional velocity, and z-directional velocity expressed as $v_z = \cos(\omega t)$.

The flow-tangency condition can be rewritten in terms of the Fourier coefficients as

$$\hat{\boldsymbol{A}} \cdot \hat{\boldsymbol{\Gamma}}_{\mathrm{b}} + \hat{\boldsymbol{B}} \cdot \hat{\boldsymbol{\Gamma}}_{\mathrm{w}} + \boldsymbol{v} \cdot \boldsymbol{n} = 0, \tag{8}$$

where $\hat{\boldsymbol{A}}$, and $\hat{\boldsymbol{B}}$ are the frequency domain AIC matrices; and $\hat{\boldsymbol{\Gamma}}_{\mathrm{w}}$ are the Fourier coefficients corresponding to the wake panels, which are just an expansion of the trailing-edge Fourier coefficients.

III. Methodology

This section presents the new methodology, which aims to provide a general reformulation of the UVLM that avoids time-stepping while capturing non-periodic components. First, we introduce the domain discretization and the parameterization, and then we present a general problem formulation that works with various types of given lifting surface kinematics.

A. Domain discretization and parameterization

The coordinates of the bound and wake mesh coordinates in the physical domain are mapped to a parametric domain Ω_0. The mapping from the parametric domain Ω_0 to the physical domain Ω is introduced by a transformation function

$$F : \Omega_0 \longrightarrow \Omega,\ \ F(\xi, \eta, t_i) = x\ , \tag{9}$$

where $\xi \in [0,\ 1]$ is the spanwise parametric coordinate, and $\eta \in \mathbb{N}$ is a time-like index in the wake vortex mesh; and x is the wake vortex coordinates in the physical domain.

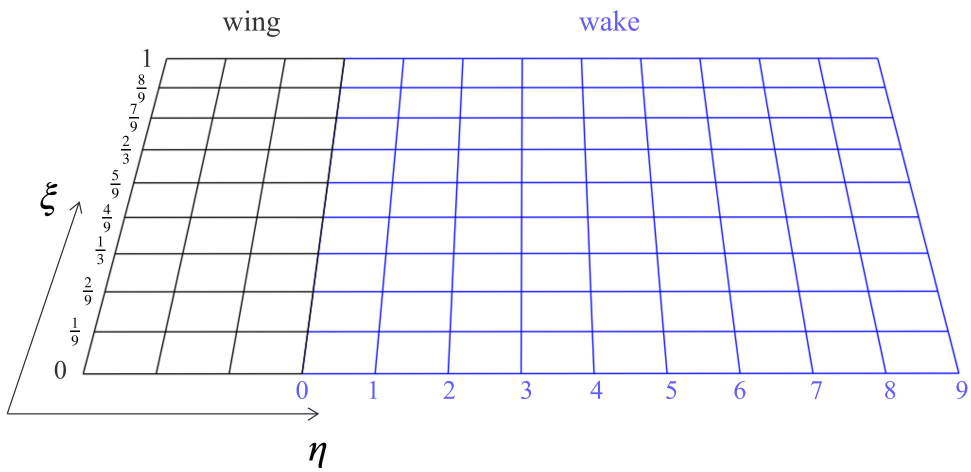

Fig. 2 Concept figure for the wake parametrization. $\xi \in [0, 1]$ **is the spanwise parametric coordinate, and** $\eta \in \mathbb{N}$ **is a time-like index in the wake vortex mesh.**

B. Problem formulations

We define a nonlinear system with the trailing edge coordinates $\overrightarrow{x}$ as the inputs. The input $\overrightarrow{x}$ is a function of the spanwise parametric coordinate ξ and the time instance t_i,

$$\overrightarrow{x(\xi, t_i)} = \begin{bmatrix} f_x(\xi, t_i) \\ f_y(\xi, t_i) \\ f_z(\xi, t_i) \end{bmatrix}\ , \tag{10}$$

where $f_x,\ f_y,\ f_z$ are functions that describe the trailing-edge kinematics at different time instance t_i. This input is defined by the user. Assuming the inertia frame has a constant velocity of (V_x, V_y, V_z), the algorithm then automatically generate the wake mesh as

$$\overrightarrow{u(\eta, \xi, t_i)} = \begin{bmatrix} D_x(\eta) f_x(\xi, t_i - \eta\Delta t) - V_x \eta \Delta t + u_x(\eta)\eta \\ D_y(\eta) f_y(\xi, t_i - \eta\Delta t) - V_y \eta \Delta t + u_y(\eta)\eta \\ D_z(\eta) f_z(\xi, t_i - \eta\Delta t) - V_z \eta \Delta t + u_z(\eta)\eta \end{bmatrix}\ , \tag{11}$$

where D_x, D_y, and D_z perturb the amplitude of the wake relative to the prescribed wake mesh, which is the history of the trailing edge motion; u_x, u_y, and u_z are additional corrections; D_x, D_y, D_z, u_x, u_y, and u_z are parameterized by B-spline control points. By setting those B-spline control points as design variables, we formulate an optimization problem to perturb the prescribed wake mesh in order to match closer to a force-free wake.

The optimization problem is expressed as

$$\begin{aligned} \textbf{minimize} \quad & \sum (v_{\text{x,ind}} - v_{\text{x,tan}})^2 + \sum (v_{\text{y,ind}} - v_{\text{y,tan}})^2 + \sum (v_{\text{z,ind}} - v_{\text{z,tan}})^2 + \\ & r_1(D_x - 1)^2 + r_2(D_y - 1)^2 + r_3(D_z - 1)^2 + r_4 u_x^2 + r_5 u_y^2 + r_6 u_z^2 \quad , \\ \textbf{with respect to} \quad & d_x,\ d_y,\ d_z,\ c_x,\ c_y,\ c_z \end{aligned} \tag{12}$$

where $v_{\text{x,ind}}$, $v_{\text{y,ind}}$, and $v_{\text{z,ind}}$ are the x, y, and z-directional component of the wake induced velocity; $v_{\text{x,tan}}$, $v_{\text{y,tan}}$, and $v_{\text{z,tan}}$ are the x, y, and z-directional component of local tangential velocities of the wake; r_1 through r_6 are the scalars that control the magnitude of the regularization terms. If their values are very large, the optimization converged to the prescribed wake geometry. The design variables d_x, d_y, d_z, c_x, c_y, c_z are the B-splines control points that parameterize D_x, D_y, D_z, u_x, u_y, and u_z, respectively.

C. Efficiency compared to the UVLM method

In this subsection, we compare the total size of the induced velocity tensor in our method with the free wake method. The reason is that the evaluation of the induced velocity is the main factor related to the computational cost of the VLM method. The induced velocity evaluated both on the bound collocation points, and the wake collocation points have to be performed at each time step for the UVLM. These induced velocities have to be computed in our method as well. Thus, we compute the total size of the induced velocity tensor in both the UVLM method and our method. The shape of the induced velocity tensor both on the bound and the wake collocation point is $[2N + 1, n_{\text{chord}} + n_{\text{wake}}, n_{\text{span}}, 3]$ in our method for one optimization iteration, where N is the domain frequencies; n_{chord} number of chordwise vortex panels; n_{span} is the spanwise vortex panels; and n_{wake} is the number of wake panel. In UVLM, the shape of the induced velocity tensor is $[n_{\text{chord}}\ (n_{\text{wake}} + 1) + \frac{n_{\text{wake}}\ (n_{\text{wake}}+1)}{2}, n_{\text{span}}, 3]$. If we assume $n_{\text{chord}} = 3$, $n_{\text{span}} = 10$, N=1, and the number of optimization iterations is 30, the size of the induced velocity tensor with respect to the number of wake panels can be computed, as shown in Fig. 3. Our method exceeds the UVLM method when the number of wake panels is greater than 175. In addition, we implement the problem such that the computation of the induced velocity is vectorized in the first dimension of the tensor shown earlier in the section. In contrast, the UVLM method usually cannot be vectorized in the time dimension.

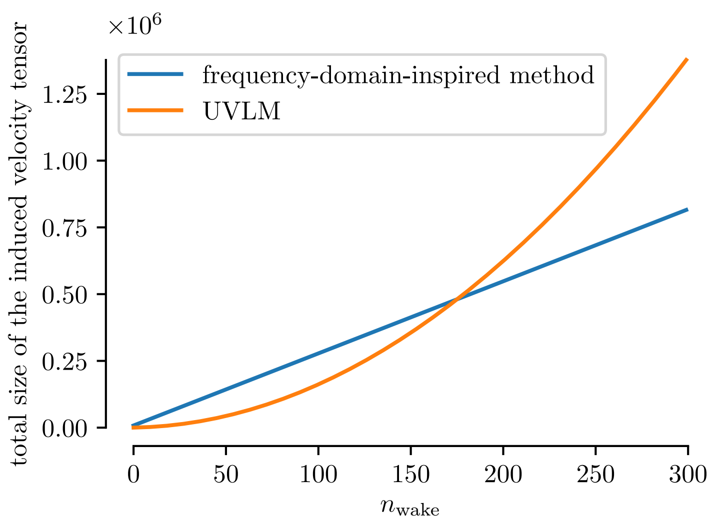

Fig. 3 Total size of the induced velocity tensor for the frequency-domain-inspired method and UVLM.

IV. Results

In this section, we first check our model with a prescribed wake geometry against a time-marching VLM model with the same prescribed wake. Then, we present two cases using the proposed approach: a rotor and a plunging wing aerodynamics analysis, allowing the wake geometry to evolve during the optimization iterations.

A. Model verification

Before allowing the wake geometry to vary across optimization iterations, we first present a verification case of a plunging wing with a prescribed wake geometry. We check the model against a time-marching VLM with the same prescribed wake geometry in this verification case. The design variable in the verification case is only the vector d_z. By having a large r_3 term of 100, the optimization converges to the same wake geometry as the prescribed wake, which is essentially the history of the trailing edge (shown in Fig. 4).

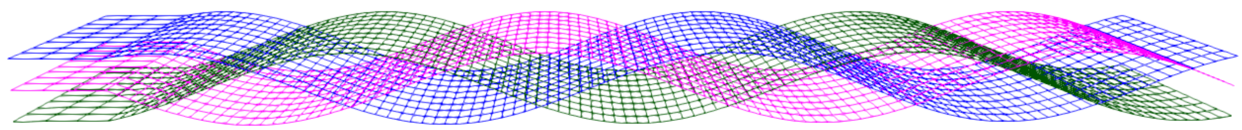

Fig. 4 Wake geometry of the plunging wing verification case. The wake geometry converges to the prescribed wake geometry with a large r_3 term as 100.

The time duration of the verification case is equal to two periods of the sinusoidal plunging motion. The amplitude of the plunging motion in the z-direction is equal to a quarter of the chord length of the wing. The lift coefficient C_{L} and the drag coefficient C_{D} computed with the frequency-domain-inspired method are checked against the time-stepping VLM with the same plunging kinematics. The results match the time-stepping VLM method well with minor differences (shown in Fig. 5).

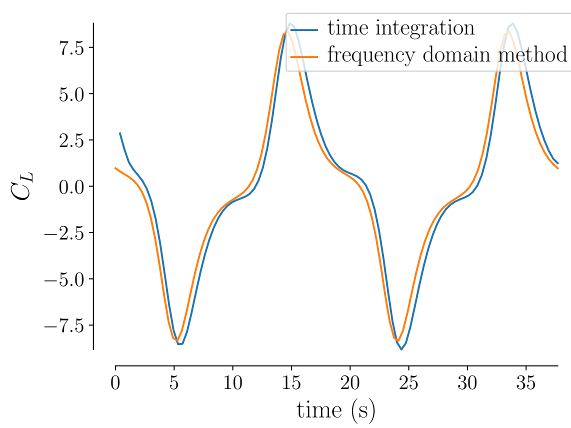

(a)

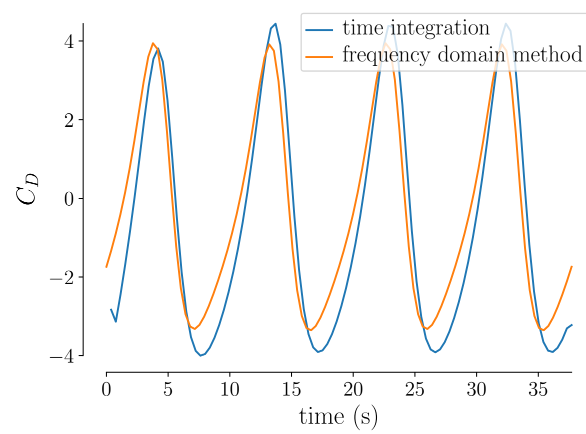

(b)

Fig. 5 Model verification against a prescribed wake time-stepping VLM model; (a) the lift coefficients C_{L}; (b) the drag coefficients C_{D}.

B. Case 1: rotary wing

1. Problem formulation

This section demonstrates the application of the new method to a rotary wing. We assume an advance ratio of 0.313, a constant pitch angle of 45°, the rotor radius R of 0.8 m, and the chord length of 0.2 m. The history of the trailing edge is given by the user. Here, we provide an example input

$$\overrightarrow{x(\xi, t_i)} = \begin{bmatrix} R\xi\cos(\omega t_i) \\ R\xi\sin(\omega t_i) \\ 0 \end{bmatrix}. \tag{13}$$

Then, the following states are generated with the algorithm:

$$\overrightarrow{u(\eta, \xi, t_i)} = \begin{bmatrix} r(\eta)\xi\cos(\omega(t_i - \eta\Delta t)) - V_x\eta\Delta t + u_x(\eta)\eta \\ r(\eta)\xi\sin(\omega(t_i - \eta\Delta t)) - V_y\eta\Delta t + u_y(\eta)\eta \\ 0 - V_z\eta\Delta t + u_z(\eta)\eta \end{bmatrix}. \tag{14}$$

Although we have perturbation terms on all x, y, and z directions of the wake geometry in the formulation, we first run an optimization with only $r_{\text{cp}}(\eta)$ as design variables, which is the B-spline control points for the radii distribution of the rotor wake along the streamwise direction. Here we set all the regularization terms to zeros. The wake geometry, and the radii distribution of the wake with respect to η is shown in Fig. 6. The contracting wake shape matches our intuition, but further verification and validation are needed. We hypothesize that the oscillation in the radial distribution is caused by the uniform parameterization of B-spline control points, which should be avoided once we have more control points in the first 50 time-like indices η. We also evaluate the thrust coefficient C_{T} as one of the parameters for aerodynamic analysis, which is shown in Fig. 7.

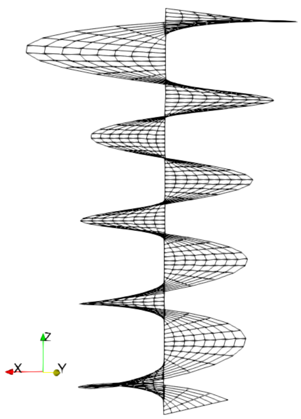

(a)

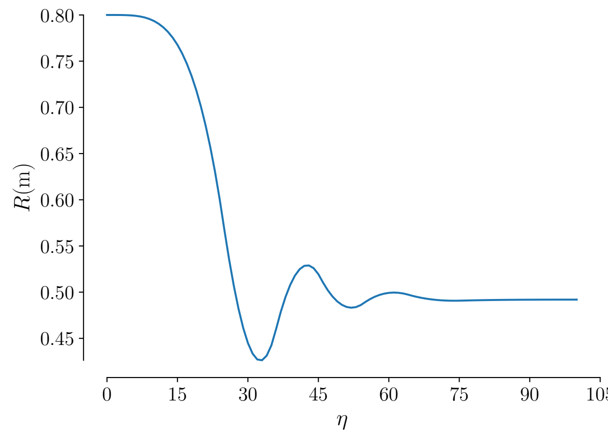

(b)

Fig. 6 Optimized wake geometry for the rotor; (a) wake geometry of the rotor; (b) the radii distribution along the streamwise time-like index η.

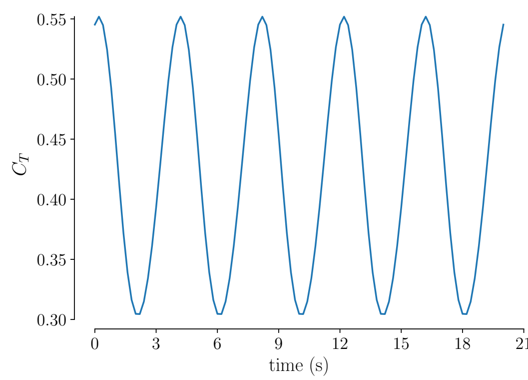

Fig. 7 Thrust coefficients over time for with the optimized rotor wake geometry.

C. Case 2: plunging wing

This section demonstrates the same approach applied to the case of a plunging wing. The wingspan B is 8 m long; and the chord length C is 2 m. The oscillation amplitude H is set to be 1.2 m. We provide a sample input, which is the trailing edge history below:

$$\overrightarrow{x(\xi, t_i)} = \begin{bmatrix} 0 \\ B\xi \\ H \sin \omega t_i \end{bmatrix}. \tag{15}$$

Equation (15) defines the kinematics of the wing as pure plunging in an inertia frame with a z-directional displacement profile $H = \sin \omega t$. The user also need to define the inertia frame velocity. Here, the inertia frame velocity is given as $[V_x, V_y, V_z] = [-1, 0, 0]$. Using the same approach defined in Sec. III, the following pattern of the states is generated:

$$\overrightarrow{u(\eta, \xi, t_i)} = \begin{bmatrix} 0 - V_x \eta \Delta t + u_x(\eta)\eta \\ b(\eta)\xi - V_y \eta \Delta t + u_y(\eta)\eta \\ h(\eta)\sin(\omega(t_i - \eta\Delta t)) - V_z \eta \Delta t + u_z(\eta)\eta \end{bmatrix}. \tag{16}$$

The first investigation is to run an optimization with only $h_{\mathrm{cp}}(\eta)$ as design variables, which are the control points for the oscillation amplitude of the rotor wake along the streamwise direction. Here we set all the regularization terms to zeros. The wake geometry, and the radii distribution of the wake along versus η are shown in Fig. 8.

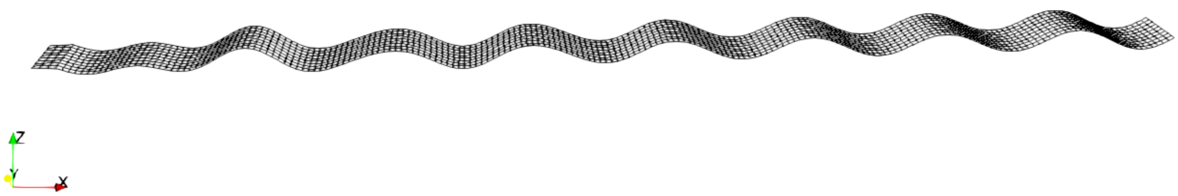

(a)

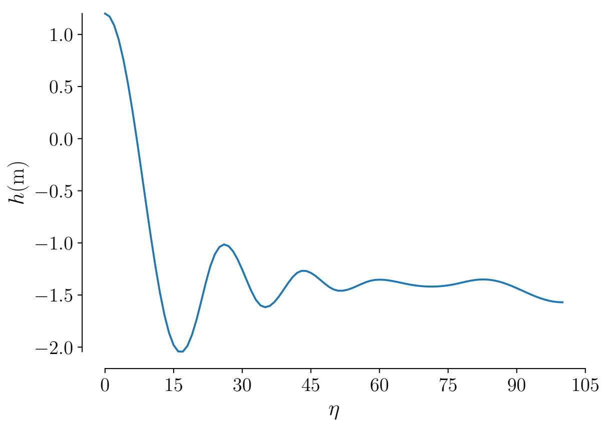

(b)

Fig. 8 Optimized wake geometry for a plunging wing; (a) wake geometry of a plunging wing; (b) the amplitude distribution along the streamwise time-like index η.

We expect an increase in the oscillation amplitude compared with the UVLM model. In addition, there should be a term that "shifts" the phase of this curve due to the induced velocity of the wake that causes the "rollup" behavior. This explains the negative values in $h(\eta)$. However, further verification and validation need to be performed in order to fully explain this phenomenon. We also evaluate the lift coefficient C_{L} and the drag coefficient C_{D} for the wing during plunging, which is shown in Fig. 9.

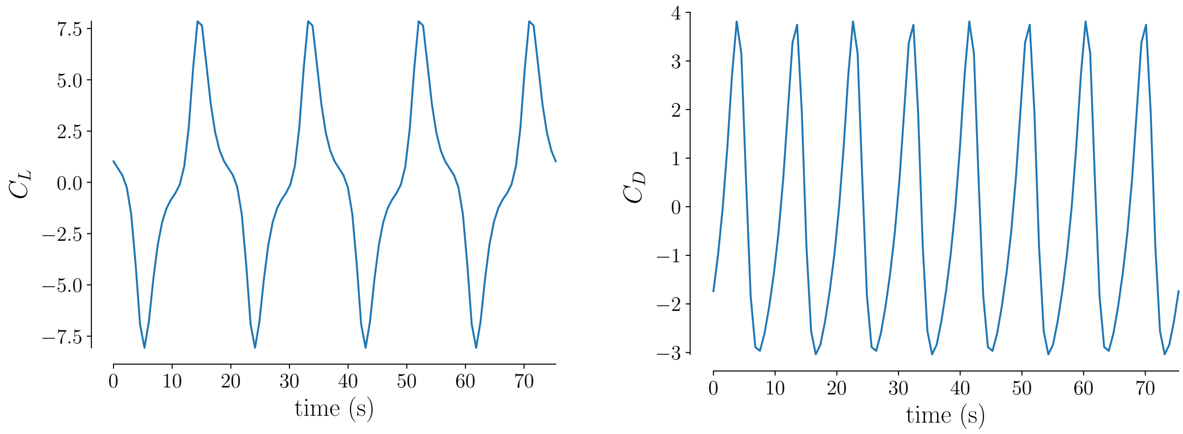

(a) **(b)**

Fig. 9 The lift coefficients C_{L} coefficients and the drag coefficients C_{D} over time with the optimized plunging wing wake geometry; (a) the lift coefficients C_{L}; (b) the drag coefficients C_{D}.

V. Conclusion and future work

We presented a method based on a frequency-domain-inspired reformulation that is general for various lifting surfaces with periodic motions, allowing the wake to deform towards a force-free direction using optimization. This method should have great potentials to be coupled with large-scale design optimization models for aerodynamic or acoustic analysis. We reviewed the time-domain VLM and the frequency domain VLM as the background of this paper in Sec. II. The methodology was then provided in Sec. III. Section IV started with a verification case of the frequency-domain-inspired model; then, aerodynamic analysis and wake geometry computation of two cases, a rotary wing case and a plunging wing case, were presented.

The method presented in this paper should lead to a promising tool for aerodynamic analysis as it has the following benefits: 1) It works well in various scenarios (e.g., rotary wings and plunging wings); 2) This method eliminates all time-stepping procedures; 3) This approach only works with a very small number of degrees of freedom.

A promising direction for future work is to apply this model to aircraft design optimization with analytical derivatives using MDO frameworks such as OpenMDAO. Further investigation and development of this method are needed, e.g., allowing the B-spline control to be a function of both η and ξ to consider the wake rollup behavior.

VI. Acknowledgments

The material presented in this paper is, in part, based upon work supported by NASA under award No. 80NSSC21M0070.

References

[1] Falkner, V., *The accuracy of calculations based on vortex lattice theory*, ARC, 1946.

[2] Anderson Jr, J. D., *Fundamentals of aerodynamics*, Tata McGraw-Hill Education, 2010.

[3] Chauhan, S. S., and Martins, J. R., "Low-fidelity aerostructural optimization of aircraft wings with a simplified wingbox model using OpenAeroStruct," *International Conference on Engineering Optimization*, Springer, 2018, pp. 418–431.

[4] Jasa, J., Martins, J. R., Chaudhuri, A., and Willcox, K. E., "Multifidelity optimization under uncertainty for a tailless aircraft," 2018.

[5] Ha, T. H., Lee, K., and Hwang, J. T., "Large-scale multidisciplinary optimization under uncertainty for electric vertical takeoff and landing aircraft," *AIAA Scitech 2020 Forum*, 2020, p. 0904.

[6] Brooks, T. R., and Smith, B. D., "Aerostructural design optimization of the D8 aircraft using active aeroelastic tailoring," *AIAA Scitech 2020 Forum*, 2020, p. 1967.

[7] Gray, J. S., Hwang, J. T., Martins, J. R. R. A., Moore, K. T., and Naylor, B. A., "OpenMDAO: An open-source framework for multidisciplinary design, analysis, and optimization," *Structural and Multidisciplinary Optimization*, Vol. 59, No. 4, 2019, pp. 1075–1104. https://doi.org/10.1007/s00158-019-02211-z.

[8] Florea, R., Hall, K. C., and Cizmas, P. G., "Reduced-order modeling of unsteady viscous flow in a compressor cascade," *AIAA journal*, Vol. 36, No. 6, 1998, pp. 1039–1048.

[9] Behbahani-Nejad, M., Haddadpour, H., and Esfahanian, V., "Reduced order modeling of unsteady flows without static correction requirement," *Journal of Aircraft*, Vol. 42, No. 4, 2005, pp. 882–886.

[10] Bundith, P., Pimanprom, P., Janthornsirijan, W., Punkun, C., Sleesongsom, S., and Bureerat, S., "Reduced-order modelling of unsteady vortex lattice method," *IOP Conference Series: Materials Science and Engineering*, Vol. 1173, IOP Publishing, 2021, p. 012040.

[11] Parenteau, M., and Laurendeau, É., "Nonlinear frequency-domain solver for vortex lattice method," *AIAA Journal*, Vol. 56, No. 6, 2018, pp. 2242–2251.

[12] Parenteau, M., and Laurendeau, E., "A general modal frequency-domain vortex lattice method for aeroelastic analyses," *Journal of Fluids and Structures*, Vol. 99, 2020, p. 103146.

[13] Fritz, T., and Long, L., "A parallel, object-oriented unsteady vortex lattice method for flapping flight," *42nd AIAA Aerospace Sciences Meeting and Exhibit*, 2004, p. 39.

[14] Egolf, T. A., and Landgrebe, A. J., "Helicopter rotor wake geometry and its influence in forward flight. Volume 1: Generalized wake geometry and wake effect on rotor airloads and performance," Tech. rep., 1983.

[15] Rosenberg, A., and Sharma, A., "A prescribed-wake vortex lattice method for preliminary design of co-axial, dual-rotor wind turbines," *Journal of Solar Energy Engineering*, Vol. 138, No. 6, 2016.

[16] Choephel, T., "Aerodynamic analysis of helicopter rotors using a higher-order, free-wake method," 2016.

[17] Katz, J., and Plotkin, A., *Low-speed aerodynamics*, Vol. 13, Cambridge university press, 2001.

[18] Miller, W. O., and Bliss, D. B., "Direct periodic solutions of rotor free wake calculations," *Journal of the American Helicopter Society*, Vol. 38, No. 2, 1993, pp. 53–60.